A Theoretical Cross-Layer Model for IEEE 802.11a-based Networks

Roger Pierre Fabris Hoefel

Resumo **—** Neste artigo é desenvolvido e validado um modelo teórico que permite analisar de maneira integrada aspectos fundamentais dos protocolos da camada física e da camada de controle de acesso ao meio empregados em redes de comunicação sem fio IEEE 802.11a.

***Palavras-Chave*—Redes locais sem fio, 802.11a, protocolos de controle de acesso ao meio, eficiência, desvanecimento.**

Abstract **—** We have derived and validated a cross-layer theoretical model in order to jointly analyze the performance of medium access control (MAC) and physical (PHY) layer protocols implemented on the IEEE 802.11a wireless local area networks (WLANs).

***Index Terms*—WLANs, 802.11a, MAC protocols, throughput, multipath fading.**

I. INTRODUCTION

Traditionally, the design issues of MAC protocols have been investigated assuming few constraints on the physical layer. In fact, most of them have assumed an ideal noiseless channel. However, the demand of spectral efficiency has driven the development of a cross-layer design methodology [1]. A conceptualization of this methodology applied to the design of state-of-art wireless networks can be found in [2-3]. In these papers it is developed an analytical model, considering a network loaded with only two stations (STAs) that generate deterministic traffic, in order to investigate the effects of fragmentation and signal-to-noise ratio (SNR) per bit on the IEEE 802.11a performance. Performance analyzes of wireless networks that take into account the jointly operation of MAC protocols, scheduling schemes, forward error correcting (FEC) coding and advanced PHY layer techniques (as multiuser detection and bi-dimensional Rake receivers) can also be found in [4-5].

Following the above mentioned cross-layer design trend, this contribution is divided as follows. We present at sections II and III a brief description of the IEEE 802.11a MAC and PHY layers, respectively. We develop at Section IV a theoretical model in order to jointly estimate the performance of 802.11a distributed coordination function (DCF) MAC and PHY layer protocols over additive gaussian noise (AWGN) and Rayleigh fading channels. A comparison between analytical and simulation results is done at Section V. The final remarks and future research directions are carried out in Section VI.

Finally, we remark that an analytical model to evaluate the IEEE 802.11b performance on noiseless channels has been developed in [6]. Hence, this paper extends significantly our previous contribution in order to theoretically analyze the performance of the IEEE 802.11a WLANs on AWGN and Rayleigh channels.

Roger Pierre Fabris Hoefel, Department of Telecommunications Engineering, University La Salle (UNILASALLE), Canoas, Rio Grande do Sul, Brazil, E-mail: roger@lasalle.tche.br

II. The IEEE 802.11a DCF MAC STATE MACHINE

We assume an *ad hoc network,* so it is used the DCF MAC state machine specified at the IEEE 802.11 Wireless Local Area Network Medium Access Control and Physical Layer Specifications [7]. The DCF provides a best-effort service similar to those ones supported by the Carrier Sense Multiple Access/Collision Detect (CSMA/CD) MAC protocol implemented on wired Ethernet LANs (i.e. IEEE 802.3) operating at 10 Mbps half-duplex mode [8, pp. 46].

This paper focuses on the IEEE 802.11a physical layer specifications [9]. The IEEE standards 802.11, 802.11a, 802.11b, and 802.11g use, with minor modifications, the same MAC layer protocols. To accomplish it, a MAC service unit (MSDU) is segmented into a MAC protocol data unit (MPDU) that, in its turn, it is mapped to the physical layer using a standardized physical layer convergence procedure (PLCP).

In order to provide a common background to the reader not familiarized with the IEEE 802.11 group of specifications, we present a description of fundamental aspects of the IEEE 802.11 MAC Management Information Base (MIB).

The 802.11 MAC coordination function can operate in the following modes [6],[10, pp. 23]:

1) *Carrier Sense Multiple access with collision avoidance (CSMA/CA)*: It is a contention-based protocol similar to the IEEE 802.3 Ethernet. Physical carrier sensing and virtual carrier-sensing functions are implemented to manage this process. The virtual carrier sensing is implemented by the Network Allocation Vector (NAV). This timer, which is updated by a control field transmitted in data and control frames, sets the amount of time that the channel will be reserved to permit uninterrupted atomic transmissions. This mandatory mode is known as DCF. It can be used in Infrastructure Base Service Set (IBSS) networks, where access points (APs) and wired backbones are implemented, and in Independent BSS (or ad hoc) networks;
2) *Priority-based access*: It is a pooling protocol that provides contention-free services in order to supply quality of-service (QoS) to time-bounded applications in IBSS networks. This optional model is labeled in the specification as the point coordination function (PCF) protocol.

The two modes are used alternately in time, i.e. a contention-free period allowed by the PCF is followed by a contention period of the DCF. The current commercial implementations of 802.11b (also known as WiFi or Wireless Fidelity) and 802.11a have focused on the DCF operational mode. The PCF limitations (e.g. the unpredictable start time of beacon frames

that announce the contention free period) have driven the developing of the IEEE 802.11e, i.e. a new MAC state machine that implements QoS polices in WLANs [11].
The DCF has the following distributed access polices [6],[10, pp. 31]:

1) *Basic positive acknowledgment (Fig. 1):* The STA only accesses the channel after implementing the physical carrier-sensing and virtual carrier-sensing functions. If the NAV is zero, then the transmission can begin immediately if the channel has been idle for longer than the DCF interframe spacing (DIFS). If the channel is busy, the station must backoff its transmission until the channel becomes idle for the DIFS period. After this DIFS period, the station: *(i)* it starts to treat the channel in units of time slot; *(ii)* it implements a binary exponential backoff period (EBP) to determine the time slot access time; *(iii)* it continues to check the channel to verify if it is busy or idle; (iv) it decrements the EBP while the channel is idle. If the channel remains idle when the EBP becomes zero, then the STA starts its MPDU transmission. Otherwise, the decrement of backoff interval stops and only resumes after the channel is detected idle for the DIFS period. The STAs exchange data based on a stop-and-go scheme: the receiver station must transmit an acknowledgment (ACK) control frame (or piggybacking ACK control information in an unicast MPDU frame) after a short interframe spacing (SIFS) period. If either the MPDU frame or the ACK control frame is corrupted or the timeout expires, then the sender station must use the extended interframe spacing (EIFS) instead of the DIFS to reschedule the time to begin a new physical channel sensing procedure. It is again used a binary EBP to set the time slot, but the contention window (CW) is doubled at each unsuccessful transmission. The CW is reset after a successful transmission. The data frame is dropped after a preestablished number of transmission attempts [12, pp. 232].

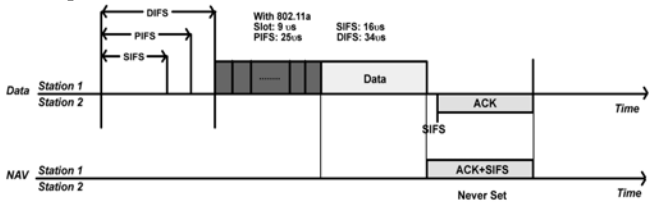

Fig. 1. Atomic basic positive ACK of data.

2) *Request to Send/Clear to Send (RTS/CTS) clearing technique (Fig. 2):* It is used to avoid the hidden terminal problem. This scheme is used to gain the control of the channel for frames larger than the RTS threshold. Initially, the same procedure used to transmit a MPDU frame in the basic positive ACK scheme must be accomplished, but now it is implemented to transmit a RTS control frame. If the RTS frame transmission is successful, the peer STS sends a CTS control frame to confirm the reservation. After that, it is transmitted a data unicast frame as in the basic positive ACK scheme. Again, the sender STS must use the EIFS to set the time for new physical channel sensing if either data or control frames are corrupted or due to the timeout of timer that controls the maximum expected delay of the CTS control frame.

Some parameters interrelated with the DCF protocol when it is used the 802.11a PHY layer are: t_{slot}*=9 μs*; *SIFS=16 us*; *DIFS=34 us*, *minimum contention window (CWmin) of 15 time slots*; *maximum CW (CWmax) of 1023 time slots*.

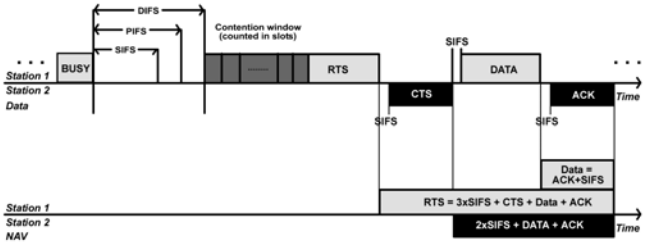

Fig. 2. The clearing technique used at atomic RTS/CTS scheme.

III. The IEEE 802.11a PHYSICAL LAYER

In this paper we follow the *Wireless LAN Medium Access Control (MAC) and Physical Layer (PHY) Specifications: High-Speed Physical Layer in the 5 GHz Band* [9], which supports transmission rates from 6 Mbps up to 54 Mbps operating in the United States of America (US) 5 GHz Unlicensed National Information Infrastructure (U-NII) band.
The IEEE 802.11a is based on Orthogonal Frequency Division Modulation (OFDM) using a total of 52 subcarriers, of which 48 subcarriers carry actual data and four subcarriers are pilots that facilitate coherent detection. The OFDM symbol interval, *tSymbol*, is set to 4μs. Therefore, the channel symbol rate R_s is of *12 Msymbols/sec*.
Fig. 3 shows the PLCP Protocol Data Unit (PPDU) of the IEEE 802.11a. As *tSymbol*= 4μs, then: *(1)* the PLCP preamble duration, *tPCLPPreamble*, is equal to 16 μs; (2*)* the PCLP field duration, *tPCLP_SIG*, is equal to 4 μs. Notice that both MPDU frames and RTS, CTS and ACK control frames are encapsulated in PPDU as shown at Fig. 3.

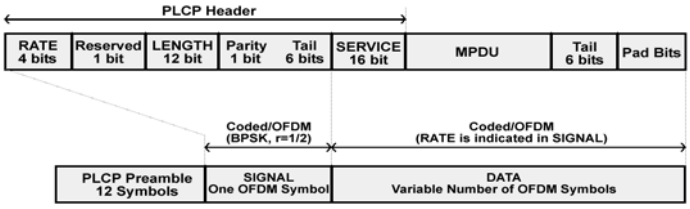

Fig. 3 –PPDU frame format of the IEEE 802.11a [9, pp.7].

Tab. 1 shows the OFDM PHY characteristics, where *BpS* means Bytes per Symbol. For instance, the *PHY mode 1* carries 3 bytes per symbol, i.e. 6 Mbps* *tSymbol/8.0=3 BpS.*

Tab. 1. The IEEE 802.11a PHY modes [2].

Mode m	*Modulation*	*Code Rate*	*Data Rate*	*BpS*
1	BPSK	1/2	6 Mbps	3
2	BPSK	3/4	9 Mbps	4.5
3	QPSK	1/2	12 Mbps	6
4	QPSK	3/4	18 Mbps	9
5	16-QAM	1/2	24 Mbps	12
6	16-QAM	3/4	36 Mbps	18
7	64-QAM	2/3	48 Mbps	24
8	64-QAM	3/4	54 Mbps	27

The RTS and CTS control frames must be transmitted at one of the rates of the basic service set (BSS) so that they can be decoded by all the STSs in the same network. The mandatory BSS basic rate set is {6 Mbps, 12 Mbps, 24 Mbps}. The ACK control frames must be transmitted using the BSS basic rate

that is less than or equal to the rate of the data frame it is acknowledging. For instance, assuming that a data frame is transmitted at the rate of 9 Mbps, the corresponding ACK frame will be transmitted at 6 Mbps.

The convolutional encoders use the industry-standard generator polynomials, $\boldsymbol{g_0}=(133)_8$ and $\boldsymbol{g_1}=(171)_8$, of rate $r=1/2$ and constrain length $K=7$ [9, pp.16]. The transfer function, using the data tabulated in [13], is given by

$$T(D) = 11D^{10} + 38D^{12} + 193D^{14} + 1331D^{16} + 7275D^{18} + 40406D^{20} + 234969D^{22} + \cdots . \quad (1)$$

The higher code rates of 2/3 and 3/4 are obtained by puncturing the original rate-1/2 code [9, pp.18].

In this contribution we investigate an IEEE 802.11a-based network that implements the mandatory BSS basic rate set, i.e. PHY modes 1, 3 and 5. The duration of RTS and CTS frames are given by (2) and (3), respectively. As shown at Fig. 3, that the *SERVICE* field has 16 bits and that 6 tail bits are used to return the convolutional code to the "zero state". In this paper, we assume, without losing the generality, that the RTS and CTS control frames are transmitted using the *PHY mode 1* ($m_{rts}=m_{cts}=1$). As the RTS and CTS have $l_{rts}=20$ *bytes* and $l_{cts}=14$ *bytes*, respectively [10, pp 61-63], then $T_{rts}(1)=50.33\ \mu s$ and $T_{cts}(1)=46.33\ \mu s$.

$$T_{rts}(m_{rts}) = tPCLP\,\mathrm{Pr}eamble + tPCLP\_SIG + \left\lceil \frac{l_{rts} + (16+6)/8}{BpS(m_{rts})} \right\rceil tSymbol . \quad (2)$$

$$T_{cts}(m_{cts}) = tPCLP\,\mathrm{Pr}eamble + tPCLP\_SIG + \left\lceil \frac{l_{cts} + (16+6)/8}{BpS(m_{cts})} \right\rceil tSymbol . \quad (3)$$

Correspondingly, to transmit a MPDU with a payload of l *octets* over the IEEE 802.11a using the *PHY mode m*, the transmission period is given by (4). The MPDU header and the cyclic redundant checking (CRC) fields have together a length of 34 bytes [10, pp. 52]. The ACK transmission time, whose length is of $l_{ack}=14$ *bytes* [10, pp. 64], is given by (5) assuming a *PHY mode m'*. In this paper $m=m'$ since we only implement the BSS basic rate set.

$$T_{mpdu}(m) = tPCLP\,\mathrm{Pr}eamble + tPCLP\_SIG + \left\lceil \frac{l + 34 + (16+6)/8}{BpS(m)} \right\rceil tSymbol . \quad (4)$$

$$T_{ack}(m') = tPCLP\,\mathrm{Pr}eamble + tPCLP\_SIG + \left\lceil \frac{l_{ack} + (16+6)/8}{BpS(m')} \right\rceil tSymbol . \quad (5)$$

IV. THROUGHPUT THEORETICAL ANALYSIS OF NETWORKS BASED ON THE IEEE 802.11a DCF

A. Analytical results for the net throughput (goodput)

We assume that the STSs generate Poisson traffic at an infinitesimally small rate resulting in a normalized offered traffic load G. Postulating a homogenous propagation delay a, the net throughput (or goodput) using the *PHY mode m* can be stated as the ratio of the average amount of time that a MPDU payload is transmitted with success, $T_{mp}(m)$, to the average cycle time $\overline{T}(m,m')$, i.e.

$$S = \frac{T_{mp}(m) S_{tx}(m,m')}{\overline{T}(m,m')}, \quad (6)$$

where $S_{tx}(m,m')$ is the probability that the transmission cycle is successful. It depends on the *PHY mode m* used to transmit the MPDU and on the *PHY mode m'* used to transmit the ACK control frame.

The time necessary to transmit a MPDU payload with l *octets* when it is used the *PHY mode m* is given by (see Tab. 1):

$$T_{mp}(m) = \frac{l}{BpS(m)} tSymbol . \quad (7)$$

In the following, avoiding a cumbersome notation, the dependence of MAC and PHY parameters with the *PHY mode* used must be implicit contextually.

Firstly, as shown at Fig. 1, we consider that the atomic data transmission consists of a basic ACK of data. Therefore, assuming Poisson traffic, the probability that the transmission cycle is successful is given by

$$S_{tx}(m,m') = e^{-aG} S_{mpdu} S_{ack} , \quad (8)$$

where S_{mpdu} and S_{ack} denote, respectively, the probability that the MPDU and ACK control frame be transmitted with success. The dependence of the success probability with receiver structure and channel model is modeled at subsection C.

The average cycle time is given by

$$\overline{T}(m,m') = \overline{B}_S + \overline{B}_{f1} + \overline{B}_{f2} + \overline{B}_{f3} + \overline{I}, \quad (9)$$

where the expected value of the idle period (i.e. the time interval between the end of a busy period and the next packet arrived) is given by $\overline{I} = 1/G$. We observe that the time that these cycles start are renewal points since the packet arriving process is memoryless.

The average busy time when the transmission is successful is given by:

$$\overline{B}_S = e^{-aG} S_{mpdu}\, S_{ack} \left[DIFS + T_{mpdu}(m) + a + SIFS + T_{ack}(m') \right]. \quad (10)$$

The capture effect is neglected in such way that the lost of frames due to collisions is independent of the lost of frames due to noise and interference. Thus, $\overline{B}_{f1}$ models the average amount of time that the channel is busy due to a collision. $\overline{B}_{f2}$ and $\overline{B}_{f3}$ model the average lost time due to unsuccessful transmission of data and ACK control frames, respectively.

$$\overline{B}_{f1} = \left[1 - e^{-aG}\right] \left[DIFS + T_{mpdu}(m) + \overline{Y} \right]. \quad (11)$$

$$\overline{B}_{f2} = e^{-aG} \left[1 - S_{mpdu}\right] \left[DIFS + T_{mpdu}(m) \right]. \quad (12)$$

$$\overline{B}_{f3} = e^{-aG} S_{mpdu} \left[1 - S_{ack}\right] \left[DIFS + T_{mpdu}(m) + a + SIFS + T_{ack}(m') \right]. \quad (13)$$

Based on the classical procedure proposed on the performance analyses of non-persistent CSMA [14], Y is defined as a random variable (RV) that models the superposition of packets during the vulnerable period a (see

Fig. 4). Consequently, the probability that no packet arrives at the interval *a-y conditioned that a collision has occurred* is given by:

$$F_Y(y/C) = \frac{e^{-G(a-y)}}{1-e^{-aG}} \quad for\ 0 \le y \le a \cdot \tag{14}$$

Therefore, the average time between the first and the last packet transmission supposing that a *collision happened during a busy period* is given by:

$$\overline{Y} = \frac{1}{1-e^{-aG}}\left(a - \frac{1-e^{-aG}}{G}\right). \tag{15}$$

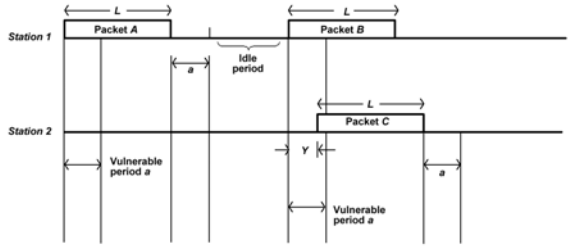

Fig. 4. Simultaneous transmissions in the vulnerable period *a*.

When it is used the RTS/CTS clearing technique, as illustrated at Fig. 2, the net throughput is still modeled by (6). However, the probability that the transmission cycle is successful is given by

$$S_{tx}(m,m') = e^{-aG} S_{rts} S_{cts} S_{mpdu} S_{ack}\,, \tag{16}$$

where S_{rts} and S_{cts} denote, respectively, the probability that the RTS and CTS control frames be transmitted successfully.
The average cycle time for RTS/CTS scheme is given by

$$\overline{T}(m,m') = \overline{B}_s + \overline{B}_{f1} + \overline{B}_{f2} + \overline{B}_{f3} + B_{f4} + B_{f5} + \overline{I}, \tag{17}$$

where the mean value of the idle period is given by $\overline{I} = 1/G$.
The expected duration of a successful atomic data transmission is given by:

$$\overline{B}_s = e^{-aG} S_{rts} S_{cts} S_{mpdu} S_{ack} \left[DIFS + T_{rts}(m_{rts}) + a + SIFS + T_{cts}(m_{cts}) + a + SIFS + T_{mpdu}(m) + a + SIFS + T_{ack}(m')\right], \tag{18}$$

In the RTS/CTS transmission mode, $\overline{B}_{f1}$, models the average amount of time in which the channel is busy due to collisions at the transmission of RTS control frames, whereas $\overline{B}_{f2}$, $\overline{B}_{f3}$, $\overline{B}_{f4}$ and $\overline{B}_{f5}$ model the average time that the channel is busy with unsuccessful transmissions, due to noise and interference, of RTS, CTS, data and ACK frames, respectively.

$$\overline{B}_{f1} = \left[1 - e^{-aG}\right] \left[DIFS + T_{rts}(m_{rts}) + \overline{Y}\right]. \tag{19}$$

$$\overline{B}_{f2} = e^{-aG}\left[1 - S_{rts}\right]\left[DIFS + T_{rts}(m_{rts})\right]. \tag{20}$$

$$\overline{B}_{f3} = e^{-aG} S_{rts}\left[1 - S_{cts}\right]\left[DIFS + T_{rts}(m_{rts}) + a + SIFS + T_{cts}(m_{cts})\right] \tag{21}$$

$$\overline{B}_{f4} = e^{-aG} S_{rts} S_{cts}\left[1 - S_{mpdu}\right]\left[DIFS + T_{rts}(m_{rts}) + a + SIFS + T_{cts}(m_{cts}) + a + SIFS + T_{mpdu}(m)\right]. \tag{22}$$

$$\overline{B}_{f5} = e^{-aG} S_{rts} S_{cts} S_{mpdu}\left[1 - S_{ack}\right]\left[DIFS + T_{rts}(m_{rts}) + a + SIFS + T_{rcs}(m_{cts}) + a + SIFS + T_{mpdu}(m) + a + SIFS + T_{ack}(m')\right]. \tag{23}$$

B. Analytical results for the frame success probability

We consider that the convolutional FEC is decoded using hard-decision Viterbi decoding and we also postulate independent errors at the channel input.
Eq. (24) models the probability of incorrectly selecting a path within an even Hamming distance *d*. The used notation emphasizes the dependence of P_d with the received signal-to-interference-plus-noise (SINR) per bit γ_b, and the *PHY mode m* [3], [15, pp. 247], [16]. The bit error rate (BER) for the *PHY mode m* modulation scheme is denoted by ρ_m.

$$P_d(\gamma_b, m) = \frac{1}{2}\binom{d}{d/2} p_m^{d/2}(1-\rho_m)^{d/2} + \sum_{k=d/2+1}^{d}\binom{d}{k}\rho_m^k(1-\rho_m)^{d-k}. \tag{24}$$

Using the transfer function defined in (1), then the union bound on the probability of decoding error (i.e. the first-event error probability) is given by

$$P_e(\gamma_b, m) < 11\,P_{10}(\gamma_b, m) + 38\,P_{12}(\gamma_b, m) + 193\,P_{14}(\gamma_b, m) + \cdots \tag{25}$$

Postulating independent errors at the input and inside of the hard decision Viterbi decoding scheme, then the upper bound of successful frame transmission of a frame with *l octets* is given by (26).

$$S(l, \gamma_b, m) < \left[1 - 8l P_e(\gamma_b, m)\right]. \tag{26}$$

If the errors inside of the decoder are interdependent, then *Pursley* and *Taipale* have shown that the upper bound of the successful frame transmission is given by [17]:

$$S(l, \gamma_b, m) < \left[1 - P_e(\gamma_b, m)\right]^{8l}. \tag{27}$$

The PCLP header is always transmitted using PHY mode 1 (see Fig. 3), then, using (27), the successful MPDU transmission is given by

$$S_{mpdu}(l, \gamma_b, m) = S(24/8, \gamma_b, 1)\, S(34 + (16+6)/8 + l, \gamma_b, m). \tag{28}$$

Correspondingly, the RTS, CTS and ACK control frames success probabilities are given by (29), (30) and (31), respectively. We again point out that in this paper it has been assumed that *m=1* for RTS and CTS control frames and *m'=m* for ACK control frame.

$$S_{rts}(l, \gamma_b, m) = S(24/8, \gamma_b, 1)\, S(20 + (16+6)/8, \gamma_b, m). \tag{29}$$

$$S_{cts}(l, \gamma_b, m) = S(24/8, \gamma_b, 1)\, S(14 + (16+6)/8, \gamma_b, m). \tag{30}$$

$$S_{ack}(l, \gamma_b, m') = S(24/8, \gamma_b, 1)\, S(14 + (16+6)/8, \gamma_b, m'). \tag{31}$$

C. Analytical results for the BER

For an AWGN the average BER for BPSK and QPSK signaling is given by [18, pp. 254, 266]

$$\rho_1 = Q\left(\sqrt{2\gamma_b}\right), \tag{32}$$

where Q(x) is the complementary Gaussian cumulative distribution function.
For rectangular M-ary quadrature amplitude modulation (QAM) with an even number of symbols over AWGN channel, the symbol error rate can be obtained by (33-35).

"$P_{\sqrt{M}}$ is the probability of error of an $\sqrt{M}$ - *ary* Pulse Amplitude Modulation system (PAM) with one-half the average power in each quadrature component of the equivalent QAM system [18, pp. 278]. Using Gray coding then the BER for QAM over AWGN is approximately given by (35).

$$\overline{P}_M(\gamma_b) = \left[1 - P_{\sqrt{M}}(\gamma_b)\right]. \quad (33)$$

$$P_{\sqrt{M}}(\gamma_b) = 2\left(1 - \frac{1}{\sqrt{M}}\right) Q\left(\sqrt{\frac{3\log_2(M)\gamma_b}{M-1}}\right). \quad (34)$$

$$\overline{P_e}(m)|_{m=5} = \rho_5 \cong \frac{\overline{P}_M(\gamma_b)}{\log_2(M)} = \frac{\overline{P}_{16}(\gamma_b)}{\log_2(16)}. \quad (35)$$

Considering a maximum ratio combining (MRC) matched with the channel diversity and that the same average power Ω is received at each diversity branch, then the probability distribution function (pdf) of the SINR per bit at the output of a MRC receiver is of gamma kind [5], i.e.

$$p(\gamma_b) = \frac{1}{\Gamma(L\,m)}\left(\frac{m}{\bar{\gamma}_b}\right)^{L\,m} (\gamma_b)^{L\,m-1} \exp\left(-\frac{m\,\gamma_b}{\bar{\gamma}_b}\right) \quad if\ \ \gamma_b > 0,\ m \geq 0.5, \quad (36)$$

where $\bar{\gamma}_b$ is the average SINR per bit at the receiver output and L is the number of diversity branches.

The average BER for BPSK signaling is given

$$\overline{P_e}(m)|_{m=1} = \rho_1 = \int_0^\infty Q\left(\sqrt{2\,\gamma_b}\right) p(\gamma_b) d\gamma_b. \quad (37)$$

The average BER for QPSK signaling over a Nakagami-m channel can also be obtained using (37) [18, pp. 269].

Closed expressions to assess the QAM signaling performance over for flat fading Rayleigh channel can be found in [19]. We notice that the consistence procedure used in the development of the IEEE 802.11 C^{++} simulator has lead to a complete agreement with the results shown at Fig. 1 of [19].

V. THEORETICAL AND SIMULATION RESULTS

The IEEE 802.11a MAC and PHY layer simulator (i.e. an integrated system level and link level simulator) implemented in this paper has the following main characteristics:

- It is assumed an ad-hoc network, as such as the DCF MAC protocol is used. The propagation time is set to *4μs* (i.e outdoor WLAN with raddi of *1200 m*) [20].
- Each STS generates Poisson MAC MSDU at rate of 13.89 packets/sec and payload of 576 bytes, i.e. a data rate of 64 kbps.
- It is implemented the MAC state machine that fulfills the atomic basic positive ACK of data transmission mode (Fig. 1) and RTS/CTS clearing technique (Fig. 2) specified at the IEEE 802.11 MIB. The CW resolution is not implemented (i.e. the packets are dropped after the first non-successful transmission attempt) in order that the simulated offered traffic follows the Poisson statistics, as analytically postulated at Section II.
- The OFDM PHY layer is implemented assuming perfect synchronism. The physical layer signal processing algorithms implements the maximum-likelihood hard decision detection of the PHY mode 1 (BPSK), PHY mode 3 (QPSK) and PHY mode 3 (16 QAM).
- The convolutional hard-decision decoding is constructed using a semi-analytic approach as follows. The average BER is estimated at a frame basis using on-line statistics collected at the demodulator output. Then the average BER is used in (27) to estimate the probability of the successful MPDU transmission. The used modular software design permits that the Viterbi convolutional decoding can be implemented as a plug-in function. This methodology, besides speeding-up the computational time, offers powerful insights on the system performance as well as on the fundamental issue of software validation.
- The Rayleigh fading is assumed both temporally independent at symbol level and independent across of the OFDM carriers.

Fig. 5 shows analytical (straight lines) and simulation (marks) results for the normalized throughput as a function of the normalized offered traffic over an AWGN channel. The labels near the marks indicate the number of STS necessary to generate a given normalized offered traffic load. The offered traffic load was normalized in relation to the symbol rate used by all PHY modes, i.e. *12 Msymbols/sec*. The normalization must be carried out after the numerical results have been calculated since traffic measurements must be done after the normalization, as in the average idle time *I*.

Besides the excellent agreement between simulation and analytical results, Fig. 5 permits to infer and ratify the following remarks: *(1)* as higher as the size of constellation used, higher the number of STSs is necessary to produce a given offered load, as theoretically expected; *(2)* the RTS/CTS overhead reduces considerably the channel efficiency (compare figures 2 and 3, please).

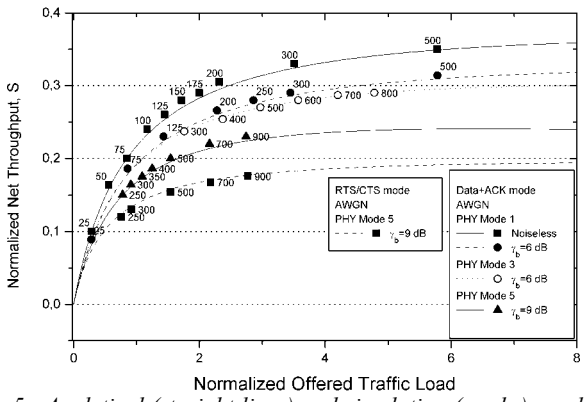

Fig. 5. Analytical (straight lines) and simulation (marks) results, of the normalized net throughput as a function of the normalized offered traffic load. AWGN channel with a=4μs.

Fig. 6 shows the average net throughput in bits per second (bps) as a function of the SINR ratio per bit at the input of the demodulator circuit. It is again assumed an AWGN channel. These results are parameterized by the PHY mode used at the physical layer and the number of STSs. Considering the parameters defined at the beginning of this section, the net offered traffic load for a system loaded with *50* and *250* STS is of *3.2 Mbps* and *16 Mbps*, respectively.

Fig. 7 is analogous to the Fig. 6, except that now it is considered a Rayleigh flat fading channel. A minor mismatched between simulation and analytical results for QAM signaling is observed. However, this phenomenon is easily explained by the well-known waterfall characteristic of the curve that maps the average SINR to the BER of QAM signaling scheme with high cardinality.

Fig. 8 shows, besides indicating the agreement between theoretical and simulation results, that the use of diversity spatial with MRC technique improves substantially the system performance. It is assumed one transmitted antenna and that the same average power is received at each receiver antenna. These results, as theoretically expected, show that the net effect of increasing the number of

received antennas on the system performance follows the law of decreasing gains.

Fig. 9 is equivalent to Fig. 6, except that now it is considered a Rayleigh flat fading channel.

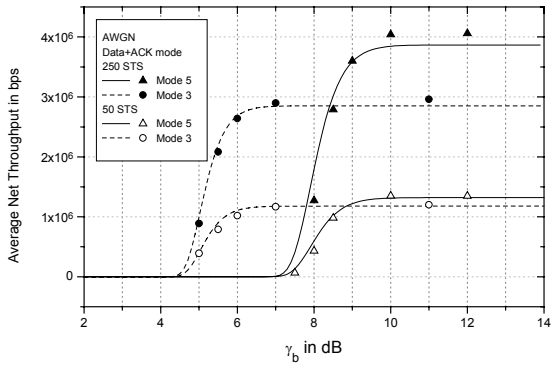

Fig. 6. Analytical (straight lines) and simulation (marks) results, of the net throughput in bps as a function of SNR per bit. AWGN channel with a=4μs.

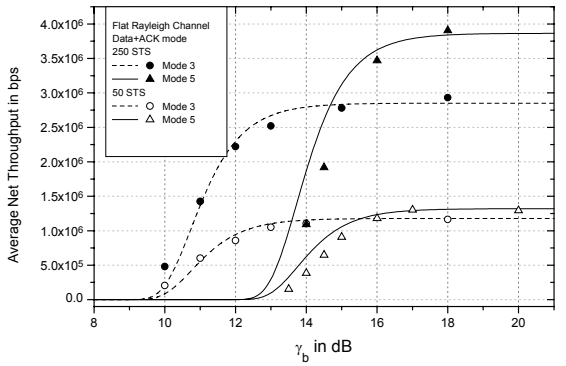

Fig. 7. Analytical (straight lines) and simulation (marks) results, of the net throughput in bps as a function of the average SNR per bit. Rayleigh flat fading channel with one degree of diversity.

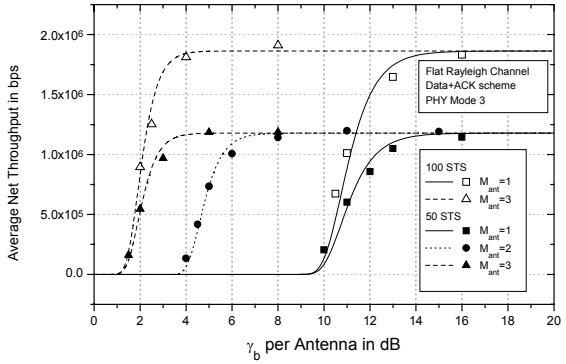

Fig. 8. Analytical (straight lines) and simulation (marks) results, of the net throughput in bps as a function of SNR per bit and the number of independent received antennas. Flat Rayleigh *channel.*

VI. FINAL REMARKS

This paper has focused on development and validation of a theoretical model that can be confidently used to analyze and to synthesize WLANs based on the IEEE 802.11a standard. The theoretical model jointly interrelates the performance of MAC and PHY protocols with system parameters (e.g. code rate, modulation scheme), traffic and channel models.

The development of theoretical models to analyze and systematize the dynamic scheduling of the IEEE 802.11a PHY mode in order to optimize the net throughput according with the system state (traffic, SNR per bit and so on) is a state of art topic that has been presently carried out.

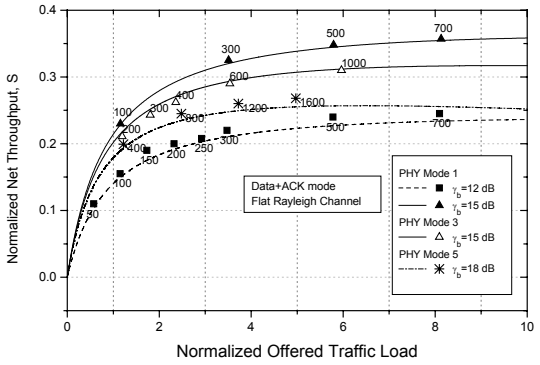

Fig. 9. Analytical (straight lines) and simulation (marks) results, of the normalized net throughput as a function of the normalized offered traffic load. Flat fading channel with one received antenna.

REFERENCES

[1] S. Shakkottai, T. S. Rappaport and P. C. Karlsson. Cross-layer design for wireless networks. *IEEE Communication Magazine,* vol. 41, no.10, pp. 74-80, Oct. 2003.

[2] D. Qiao and S. Choi. "Goodput Enhancement of IEEE 802.11 Wireless LANs via Link Adapatation". *IEEE International Conference on Communications 2001,* vol 7, pp 11-14, June 2001.

[3] D. Qiao, S. Choi and K. G Shin. "Goodput Analyzes and Link Adaptation for the IEEE 802.11a Wireless LANs*," IEEE Trans. Mobile Comuting*, pp. 278-292, 2002.

[4] R. P. F. Hoefel and C. de Almeida. "Performance of CDMA/PRMA TDD protocol with a decorrelating multiuser detector and an adaptive permission access scheme", *Electronics Letter*s, v.37, n. 15, pp. 980-981, July 2001.

[5] R. P. F. Hoefel and C. de Almeida, "Effects of Dynamic Time Slot Scheduling Schemes and Soft Handoff on the Performance of TDD DS CDMA Systems with 2D Rake Receivers", *Journal of the Brazilian Telecommunications Society*, vol. 18, no. 1, pp. 10-22, June 2003.

[6] R. P. F. Hoefel, *"*On the Performance of IEEE 802.11-based Outdoor Networks with Poisson and Self-Similar Traffic", *XX Telecommunications Brazilian Symposium, 2003*

[7] IEEE 802.11. Wireless LAN Medium Access Control (MAC) and Physical Layer (PHY) Specifications, Standard, IEEE, Aug. 1999.

[8] C. E Spurgeon. *"Ethernet –O Guia Definitvo"*. O'Reilly, 2000.

[9] IEEE 802.11a*, "Part 11: Wireless LAN Medium Access Control (MAC) and Physical Layer (PHY) Specification – Amendment 1: High-speed Physical Layer in the 5 GHz band",* supplemented to IEEE 802.11 standard, Sept. 1999.

[10] M. S. Gast, *802.11 Wireless Networks*. O'Reilly, 2002.

[11] S. Mangold, S. Choi et. al. "Analysis of IEEE 802.11 for QoS Support in WLANs", *IEEE Wireless Communications,* pp. 40-50, Dec. 2003.

[12] J. Heiskala and J. Terry, *OFDM Wireless LANs: A Theoretical and Practical Guide.* Sams Publishing, 2001.

[13] J Conan. "The Weight Spectra of Some Short Low-Rate Convolutional Codes," *IEEE Trans. Commun***,** vol. 32, pp. 1050-1053, Sept. 1984.

[14] L. Kleinrock, and F. A. Tobagi. "Packet Switching in Radio Channels: Part I – Carrier Sense Multiple Modes and Their Throughput Delay Characteristics," *IEEE Trans. on Communication,* v. 23, n.12, pp. 1400-1416, July 1975.

[15] A. J. Viterbi and J. K. Omura *"Principles of digital communication and coding,"* NY: McGraw-Hill, 1979.

[16] R. P. F. Hoefel, C. de Almeida. "A comparative study on the performance of CDMA/PRMA and CDMA/ALOHA protocols with Matched Filter and Multiuser Decorrelator Receiver" (in Portuguese), XVII Telecommunications Symposium, 2000.

[17] M. B. Pursle and D. J. Taipale. "Error Probabilities for Spread-Spectrum Packet Radio with Convolutional Codes and Viterbi Decoding," *IEEE Trans. Commun***,** vol. 35, n. 1, p. 1-12, Jan. 1987.

[18] J. G Proakis, "*Digital Communications",* New York, 2001.

[19] W. T. A. Lopes, F. Madeiro and M. S. Alencar. "Closed Expression for QAM Bit Error Rate on Rayleigh Multipath Channels" (in Portuguese), *XX Telecommunications Symposium, 2003.*

[20] M. V. Clark, K. K. Leung, B. McNair and Z. Kostic, "Outdoor IEEE 802.11 Cellular Networks: Radio Link Performance," *Proc. of IEEE International Conference on Communication*, 2002.